RSC Advances

PAPER

View Article Online
View Journal | View Issue

Cite this: *RSC Adv.*, 2014, **4**, 52263

Melamine based porous organic amide polymers for CO_2 capture

Sonia Zulfiqar,[ab] Muhammad Ilyas Sarwar*[ac] and Cafer T. Yavuz*[d]

Amide based porous organic polymers were synthesized by the reaction of 1,3,5-benzenetricarbonyl trichloride with 2,4,6-triamino-1,3,5-triazine using two different solvents. Polyamide chains were derived from tri-functional monomers and their relative properties were compared in both media. These polymers were subjected to various analyses including FTIR, XRD, TGA, BET surface area and pore size analysis, FESEM and CO_2 adsorption measurements. Thermal and chemical stability was achieved through strong amide building blocks in the polymer structure. The basic ring nitrogen and amide groups in the polyamide networks had the affinity to capture CO_2. The maximum CO_2 uptake of 2.99 $cm^3\ g^{-1}$ (0.134 mmol g^{-1}) at 273 K and 1 bar was obtained with the polyamide synthesized in DMAc–NMP (PA-1), revealing better efficiency than the polyamide prepared using 1,4-dioxane (PA-2) due to higher porosity and improved surface area. These thermally stable polyamides are anticipated to be good sorbents for CO_2 capture in hostile environments.

Received 29th September 2014
Accepted 10th October 2014

DOI: 10.1039/c4ra11442f

www.rsc.org/advances

1. Introduction

As the global energy crisis becomes progressively acute, the dependence on natural gas has been economically attractive from the environmental viewpoint. Conversely, the presence of CO_2 as a non-burning component in natural gas and the burning of fossil fuels to meet the world's energy needs enhanced the emission of greenhouse CO_2.[1] The existing level of CO_2 is expected to rise from 280 ppm from the preindustrial revolution period (early 1900s) to 450 ppm by 2050 if no measure is taken to alleviate greenhouse gas emissions.[2] Therefore, CO_2 is a major greenhouse gas, which causes global warming. Improving the efficiency of energy use and increasing the use of low-carbon energy sources are considered to be potential ways to reduce CO_2 emissions.[3] Alternatively, capturing and permanently sequestering CO_2 is another way to curb greenhouse gas emissions for the improvement of quality of the environment.[4] The development of suitable CO_2 capture and sequestration technologies has become a key issue to be addressed by the scientific community. The typical technology for CO_2 removal from CH_4 is amine absorption; however, the process is energy-consuming and cost-intensive.[5] Research in this field mainly concerns several CO_2 capture technologies or methods, such as amine-based absorption, membrane-based separation, adsorption, and cryogenic separation.[6] The CO_2 adsorption has been identified as one probable solution to reduce greenhouse gas emissions.[7,8] The success of this approach is mainly dependent upon the development of a low-cost adsorbent with a high CO_2 selectivity and adsorption capacity. The adsorption of CO_2 on conventional zeolites,[9–12] activated carbons[13–15] and coals[16] have been investigated by many researchers. Because the adsorption performance of these conventional adsorbents for CO_2 could not meet the requirement of their commercial application, future applications of adsorption are still limited due to the availability of new and better adsorbents.

Recently, many research activities have been focused on the development of novel adsorbents, such as modified activated carbons and modified zeolites, by means of surface modification for enhancing CO_2 adsorption or the development of metal–organic frameworks (MOFs) for CO_2 capture. Among the porous materials, microporous organic polymers have attracted significant interest due to their potential relevance in the field of molecular separations, heterogeneous catalysis, and gas storage.[17–20] Various types of microporous organic networks have been designed and synthesized, *e.g.*, covalent organic frameworks (COFs)[21–23] are crystalline organic networks which are analogous to metal–organic frameworks (MOFs). COFs possess highest surface areas among organic porous materials but boron based COFs suffer physicochemical stability issues. The development of crystalline imine based COF have addressed this stability issue.[23] Robust covalent triazine frameworks (CTFs),[24,25] conjugated microporous polymers

[a]*Department of Chemistry, School of Natural Sciences (SNS), National University of Sciences and Technology (NUST), Islamabad 44000, Pakistan. E-mail: ilyassarwar@hotmail.com; Fax: +92-51-90855552; Tel: +92-51-90855578*

[b]*Institute for Polymer Materials, POLYMAT, University of the Basque Country (UPV-EHU), Joxe Mari Korta Center, Avda. Tolosa 72, 20018 Donostia-San Sebastian, Spain*

[c]*Department of Chemistry, Quaid-i-Azam University, Islamabad 45320, Pakistan*

[d]*Graduate School of EEWS, Korea Advanced Institute of Science and Technology, 335 Gwahangno, Yuseong-gu, Daejeon 305-701, Republic of Korea. E-mail: yavuz@kaist.ac.kr; Fax: +82-42-350-2248; Tel: +82-42-350-1718*

(CMPs),[26] porous poly(aryleneethynylene) (PAE),[27–29] porous aromatic frameworks (PAFs),[30] polymers of intrinsic microporosity (PIMs)[31] and hyper-cross-linked polymers (HCPs)[32–35] have also been reported.

Polyamides were the first engineering thermoplastics produced and are well documented as a class of high performance materials due to their implausible thermal stability and specific strengths, good chemical resistance, marvelous mechanical properties and dimensional stability over a wide range of temperature.[36,37] Unfortunately, strong intermolecular associations of polyamide chains and rigidity of structure make them intractable limiting their applicability.[36] Reduced thermoplastic fluidity and solubility in organic solvents are the chief concerns for wide applications of polyamides especially in the area of automobile, aerospace, and other related industries. Actually, chain composition and chemical configuration impart matchless thermal and dimensional stability but at the same time limit their fusibility within processing temperature and render them insoluble. Various approaches have been carried out to overcome the solubility issues making processability and fabrication facile, without compromising their thermal characteristics. Therefore, introducing kinks, meta rings, soft segments or aliphatic sequences into the main chain could improve solubility, thermal stability, also lowers T_m and prevent crystallinity of the polymer films.[38,39] In general, the hydrogen bonding capability of the amide linkages causes strong intermolecular forces which give rise to very high T_g or T_m of the polyamides. Polyamides synthesized in the present work offered more structural rigidity to the materials and therefore, are anticipated to be good candidates for CO_2 adsorption in severe environmental circumstances.

In this attempt, a relative investigation on the synthesis, characterization and reaction conditions of polyamides in two different solvents has been described. Polymer chains were synthesized by the reaction of 1,3,5-benzenetricarbonyl trichloride with 2,4,6-triamino-1,3,5-triazine separately in DMAc–NMP and in 1,4-dioxane. The effect of solvents on the condensation polymerization of polyamides and their related properties, particularly CO_2 adsorption measurements were focused. They were further characterized using Fourier transform infrared spectroscopy (FTIR), X-ray diffraction (XRD), thermogravimetric analysis (TGA), BET surface area and pore size analysis, field emission scanning electron microscopy (FESEM) and CO_2 adsorption measurements. To the best our knowledge, it is a first report on the comparative effect of solvents on the CO_2 capture capacity of polyamides.

2. Experimental

2.1. Chemicals

2,4,6-Triamino-1,3,5-triazine (Melamine) (99%), 1,3,5-benzenetricarbonyl trichloride (98%), anhydrous 1-methyl-2-pyrrolidone (NMP, 99.5%), anhydrous 1,4-dioxane (99.8%) and acetone (≥99.5%) were procured from Sigma-Aldrich and used as such. Anhydrous *N*,*N*-dimethylacetamide (DMAc, 99.8%) provided by the courtesy of Aldrich was dried over molecular sieves prior to use.

2.2. Characterization

FTIR spectra of the polyamides synthesized in DMAc–NMP mixture and 1,4-dioxane were recorded over the range 4000–550 cm^{-1} at a resolution of 4 cm^{-1} using Jasco FTIR 4100 Spectrometer. Elemental analysis was performed using a Perkin-Elmer 2400 CHN elemental analyzer. The diffraction pattern of powdered polyamide samples were recorded by a Rigaku (D/Max-2500) HR-X-ray diffractometer using Ni-filtered Cu Kα radiation at 40 kV and 300 mA. Measurements were performed for 2θ in the range of 2° to 80° with a step size of 0.01° and scan speed of 2° min^{-1}. Thermal stability of the polyamides were determined using NETZSCH TG 209 F3 thermogravimetric analyzer using 1–5 mg of the sample in Al_2O_3 crucible heated from 25 to 900 °C at a heating rate of 10 °C min^{-1} under both nitrogen and air atmosphere with a gas flow rate of 20 mL min^{-1}. Field-emission scanning electron microscopy was used to study the surface morphology of the synthesized polyamides using Nova 230 & Magellan 400 FE-SEM. A Tristar 3020, Micromeritics (USA) porosimetry analyzer was used to measure nitrogen adsorption–desorption isotherms of polyamides at 77 K. For surface area determination, Brunauer–Emmett–Teller (BET) method was used using a nitrogen molecule surface area of 0.162 nm^2. A Tristar 3000, Micromeritics (USA) CO_2 analyzer was used to determine CO_2 adsorption capacity at pressure of 1 bar. The polyamide samples were degassed at 120 °C for 6 h under vacuum prior to surface area and CO_2 adsorption analyses.

2.3. Synthesis of polyamide (PA-1)

A 1 : 1 solvent mixture comprising of 1-methyl-2-pyrrolidone (NMP) and *N*,*N*-dimethylacetamide (DMAc) was prepared. The monomer 2,4,6-triamino-1,3,5-triazine (5 mmol) was charged into a 500 mL flask equipped with a dropping funnel and a magnetic stirrer (Scheme 1). The solvent mixture was added to the flask already containing triamine with continuous stirring for complete dissolution under inert atmosphere. The monomer was dissolved in the DMAc–NMP mixture upon slight heating and then allowed to come at ambient temperature. To the amine solution, 1,3,5-benzenetricarbonyl trichloride (5 mmol) in the same solvent mixture was added drop-wise using dropping funnel with constant agitation. The polyamidation reaction is highly exothermic in nature, so in order to avoid any side reaction; the reaction flask was cooled to 0 °C for 1 h. The solution was initially transparent and bright orange in color but as reaction proceeds; the color of solution changed to golden yellow but still remained transparent. The reaction mixture was further agitated for 72 h at room temperature. The dirty white precipitates formed were isolated and washed with fresh DMAc–NMP mixture. The product was then immersed in acetone for three days during which time the acetone was decanted and freshly replenished three times. The dirty white powder was dried under vacuum at room temperature, yield (94%). The structure of polyamide synthesized in DMAc–NMP mixture was characterized by FTIR and CHN analyses. FTIR (KBr): 3307 cm^{-1} (N–H stretch), 1552 cm^{-1} (N–H bend), 1644–1666 cm^{-1} (C=N & C=O stretch), 3138 cm^{-1} (aromatic C–H

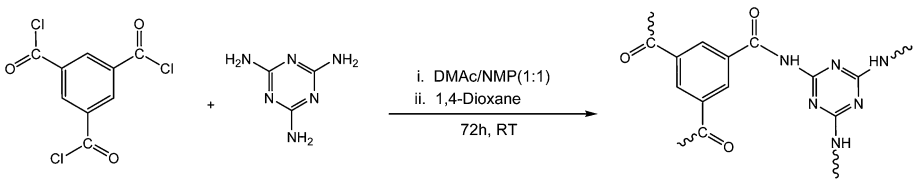

Scheme 1 Polyamidation reaction in two different solvents.

stretch), 1502 cm^{-1} (aromatic C=C stretch), 1161 cm^{-1} (C–N stretch). These vibrations indicated the condensation of monomers to yield polyamide. Elemental analysis (CHN): 51.03 %C (51.07), 2.12 %H (2.14), 29.75 %N (29.78).

2.4. Synthesis of polyamide (PA-2)

In this strategy, polyamidation reaction was performed in 1,4-dioxane medium. The solutions of 1,3,5-benzenetricarbonyl trichloride (5 mmol) and 2,4,6-triamino-1,3,5-triazine (5 mmol) were prepared separately in 1,4-dioxane. A flask containing triamine solution was kept in an ice bath and then the acid chloride solution was added drop-wise into triamine solution using dropping funnel. The reaction mixture was constantly agitated till the complete condensation of the monomers. After 72 h, stirring was stopped and the precipitates formed were found to be light pink in color. These precipitates were filtered and washed with fresh 1,4-dioxane. These were then dipped in acetone and dried under vacuum, yield (90%). Polyamide synthesized using 1,4-dioxane was characterized by FTIR and CHN analyses. FTIR (KBr): 3339 cm^{-1} (N–H stretch), 1562 cm^{-1} (N–H bend), 1668 cm^{-1} (C=N & C=O stretch), 3133 cm^{-1} (aromatic C–H stretch), 1500 cm^{-1} (aromatic C=C stretch), 1232 cm^{-1} (C–N stretch). These characteristic bands confirm the formation of the polyamide. Elemental analysis (CHN): 51.01 %C (51.07), 2.10 %H (2.14), 29.74 %N (29.78).

3. Results and discussion

Porous polymers have gained a growing interest because of their potential to blend the properties of both porous materials and polymers. They can be designed by suitably selecting the monomers to exhibit advantages of high surface area, well defined porosity, easy processability, moldable monolithic form and as thin films. In this study, we have chosen two monomers *i.e.*, melamine and 1,3,5-benzenetricarbonyl trichloride for polymerization to generate porous polyamides. Two polyamides PA-1 and PA-2 were prepared in DMAc–NMP and 1,4-dioxane solvents by condensing 2,4,6-triamino-1,3,5-triazine with 1,3,5-benzenetricarbonyl trichloride. Effect of these solvents on polymerization and CO_2 adsorption capacity of polyamides were scrutinized. The results obtained from XRD, TGA, FESEM, BET analysis and CO_2 adsorption measurements are described below.

3.1. X-ray diffraction

X-ray diffraction measurements on powdered samples of PA-1 and PA-2 are presented in Fig. 1. Both the solvents influenced XRD patterns of synthesized polyamides. Fig. 1a showed increased crystallinity of PA-1 and very sharp peaks in the diffraction pattern were observed when DMAc–NMP mixture employed as the reaction medium. This solvent system yielded more ordered structure and efficient closed packing of the synthesized polyamide chains. Many covalent organic frameworks reported have sheet like morphologies and whose XRD pattern have been modeled using stacked sheets with hexagonal network topologies.[21,40] However, the formation of strong hydrogen bonds between the amide groups of polyamide promotes non-planar, three-dimensional architectures suggesting an extended three-dimensional porous network. On the contrary, PA-2 prepared in 1,4-dioxane showed a decrease in

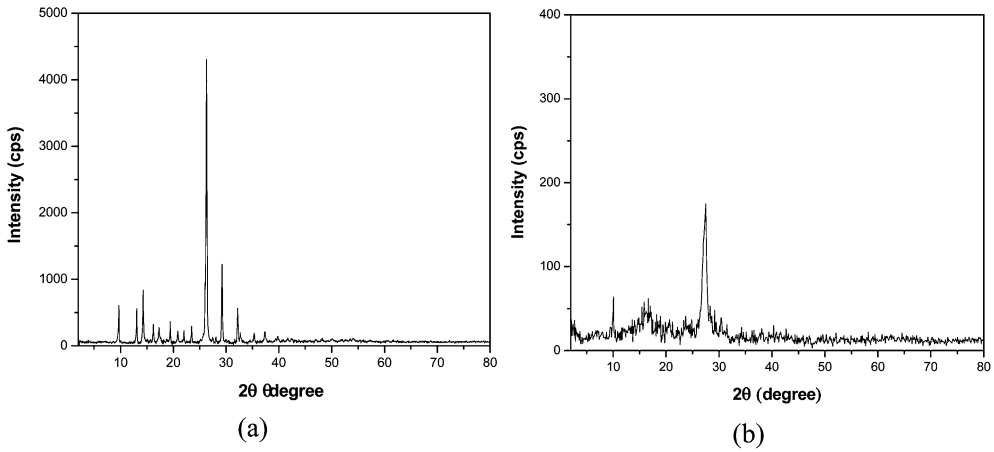

Fig. 1 XRD patterns of polyamides synthesized using (a) DMAc–NMP (b) 1,4-dioxane.

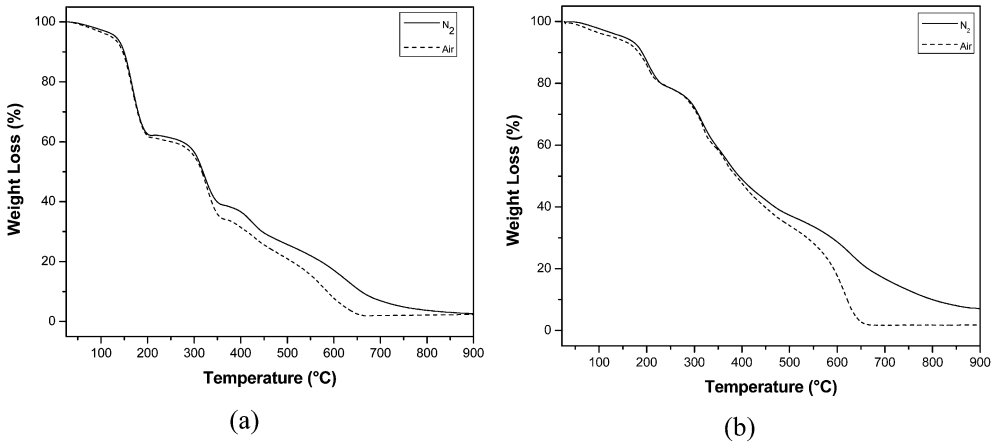

Fig. 2 TGA thermograms of polyamides synthesized using (a) DMAc–NMP (b) 1,4-dioxane.

crystallinity. Fig. 1b depicted more amorphous behavior with a broad peak around 27°. This obviously suggested a less ordered chain packing giving weak crystalline diffraction pattern.

3.2. Thermogravimetric analysis

Thermogravimetric analysis of both polyamides was carried out in N_2 and air atmospheres (Fig. 2). The evaluation of thermal stability of polyamides to be used as CO_2 adsorbents is very crucial from the view point of commercial relevance. Thermograms of PA-1 are given in Fig. 2a and this material showed a weight loss of 40% between 150 and 200 °C that might be due to entrapped solvent molecules in the pores. Further heating gave the decomposition temperature around 350 °C indicating the high thermal stability of the resulting polyamide in both the atmospheres. Fig. 2b depicted thermograms of PA-2 with initial weight loss (5%) around 200 °C due to removal of traces of solvent/moisture. The thermal decomposition temperatures of polyamides PA-1 and PA-2 were in the range of 300–350 °C and 250–350 °C respectively. PA-1 possessed better thermal stability than the PA-2 as evident from the thermal data suggesting the solvent effect on thermal stability of the resulting polyamides.

3.3. Textural characterization

The porosity of synthesized polyamides was monitored through N_2 uptake measured at 77 K to observe the influence of reaction solvents utilized for polymerization. Fig. 3 describes the N_2 adsorption isotherms for both PA-1 and PA-2 prepared in different solvents and Table 1 presents the textural parameters derived from these isotherms. Polyamide PA-1 gave BET surface area 84.5 $m^2\ g^{-1}$, Langmuir surface area 116.8 $m^2\ g^{-1}$, average pore size 13.6 nm and pore volume 0.41 $cm^3\ g^{-1}$. Polyamide PA-2 exhibited BET surface area 22 $m^2\ g^{-1}$, Langmuir surface area 28 $m^2\ g^{-1}$, average pore size 17.9 nm and pore volume 0.13 $cm^3\ g^{-1}$. The N_2 uptake for polyamide synthesized using 1,4-dioxane (PA-2) was found to be lower relative to the polyamide prepared in DMAc–NMP (PA-1). DMAc–NMP mixture proved to be good solvent system to produce more porous polyamide network structure than 1,4-dioxane. The N_2 sorption isotherms of PA-1 and PA-2 displayed "Type-II" and "Type-III" behaviors respectively. Porous polymer networks have been prepared using various monomers through solution polymerization technique in different solvents.[31] On removal of the solvent, the resulting polymer networks display permanent porosity with a broad pore

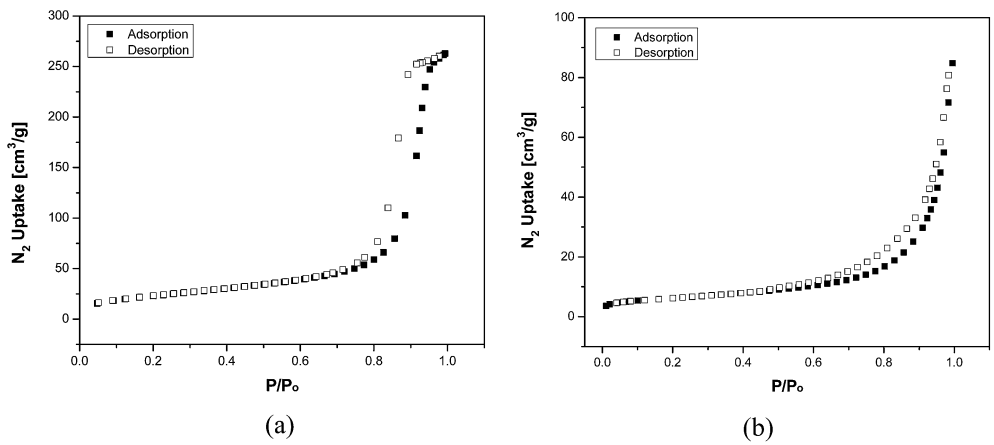

Fig. 3 N_2 isotherms for polyamides synthesized using (a) DMAc–NMP (b) 1,4-dioxane measured at 77 K.

Table 1 Textural parameters calculated from N_2 adsorption isotherms at 77 K

Parameter	DMAc–NMP	1,4-Dioxane
BET surface area ($m^2\ g^{-1}$)	84.5	22.0
Langmuir surface area ($m^2\ g^{-1}$)	116.8	28.0
Average pore size (nm)	13.6	17.9
Pore volume ($cm^3\ g^{-1}$)	0.41	0.13

size distribution ranging from micropores through mesopores (2–50 nm) to macropores (>50 nm). The porosity within polymer networks may be evolved from the trapped solvent molecules as they form, whereas the larger pores originate from phase separation of the polymer from the solvent. This direct synthesis methodology can generate pores during solution polymerization, followed by removal of the solvent from the pores. Microporous polymers with extremely high surface area and permanent porosity that persists even in the dry state can be prepared by direct synthesis procedures, for example, polymerization of rigid and contorted monomer building blocks that inhibit space-efficient packing. Here we have also used the same technique and condensed the monomers to yield the porous polymeric network structures. The resulting polyamides gave low surface areas which may be due to random orientation of the pores in the network. However, PA-2 showed long and extended network structure resulting in entangled chains as evident from XRD pattern showing a broad peak around 27°. Further, the functionality of the monomers can be increased to yield highly porous polyamides with more CO_2 uptake.

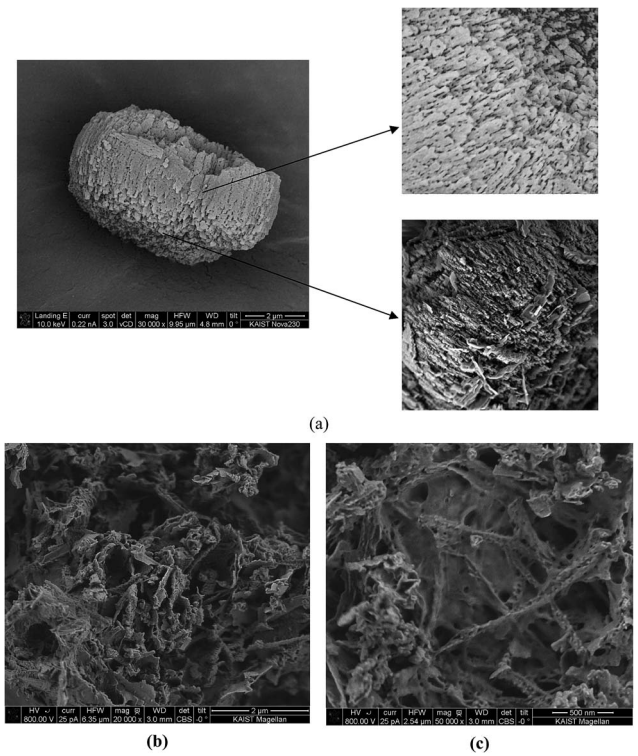

Fig. 4 FESEM micrographs of polyamides synthesized using (a) DMAc–NMP (b & c) 1,4-dioxane.

3.4. Field emission scanning electron microscopy

Morphology of polyamides was explored on the powdered samples using field emission scanning electron microscopy as shown in Fig. 4. The surface morphology of the PA-1 exhibited porosity in the sample (Fig. 4a) while PA-2 illustrated nearly non-porous structure (Fig. 4b). FESEM images of PA-1 depicted more free volume with the less compact structure, thus indicating a more porous nature of the sample. However, the micrographs of PA-2 exhibited a compact structure with less free volume clearly illustrating a non-porous morphology. The morphological analysis did support the porosity results measured through N_2 uptake rendering more porous polyamide structure, when DMAc–NMP was employed as the reaction medium.

3.5. CO_2 adsorption measurements

CO_2 adsorption isotherms were measured at 273 K and 298 K, at pressure up to 1 bar as shown in Fig. 5. The sorption of carbon dioxide at 273 K is well documented for the analysis of porous carbons.[13] The usefulness of this analysis to porous polymers has already been reported.[26] CO_2 sorption has the advantage of faster measurement times than N_2 due to the higher kinetic energy of CO_2 at 273 K compared to N_2 at 77 K. In this study, polyamides were made using two solvent systems *i.e.*, DMAc–NMP and 1,4-dioxane. Subsequently, these polymers were evaluated for their CO_2 uptake in order to confirm their ability as effective CO_2 sorbents. The highest uptake of CO_2 was found for PA-1 to be 2.99 $cm^3\ g^{-1}$ (0.134 mmol g^{-1}) at 273 K that reduced to 1.98 $cm^3\ g^{-1}$ (0.09 mmol g^{-1}) with increase in temperature to 298 K. The polyamide PA-2 indicated a lower uptake as given in Fig. 5 and Table 2 described 1.94 $cm^3\ g^{-1}$ (0.086 mmol g^{-1}) uptake of CO_2 at 273 K which decreased to 1.21 $cm^3\ g^{-1}$ (0.054 mmol g^{-1}) at 298 K. CO_2 uptake reduced substantially with rise in temperature from 273 K to 298 K, thus exhibiting the temperature dependence of adsorption capacity. CO_2 adsorption capacities of both the polyamides decreased with rise in temperature due to the exothermic nature of the binding.[41] The higher uptake of CO_2 by PA-1 relative to PA-2 may be ascribed on the basis of porosity, which is influenced by the solvent used for polymerization reaction. The effect of solvent could be explained in terms of polarity of the medium. DMAc–NMP solvent system is more polar than 1,4-dioxane and the monomers solubility is high in more polar solvent, therefore, polymerization reaction may take place swiftly in DMAc–NMP as compared to 1,4-dioxane affecting the structural packing and porosity of the resulting polyamide. The CO_2 uptake data indicated that DMAc–NMP was a good solvent mixture relative to 1,4-dioxane for polymerization and PA-1 displayed more potential towards CO_2 uptake. Apart from porosity *i.e.*, surface area, pore size and pore volume, other parameters do influence the CO_2 adsorption that include heteroatom ring nitrogen and groups having strong affinity towards CO_2 like –COO, C═O, –OH, $-NH_2$.[42] The polar sites of these groups develop strong interactions with CO_2 *via* hydrogen bonding. Polyamides have such binary interaction sites –NH and C═O. The presence of ring nitrogen's in the network of the

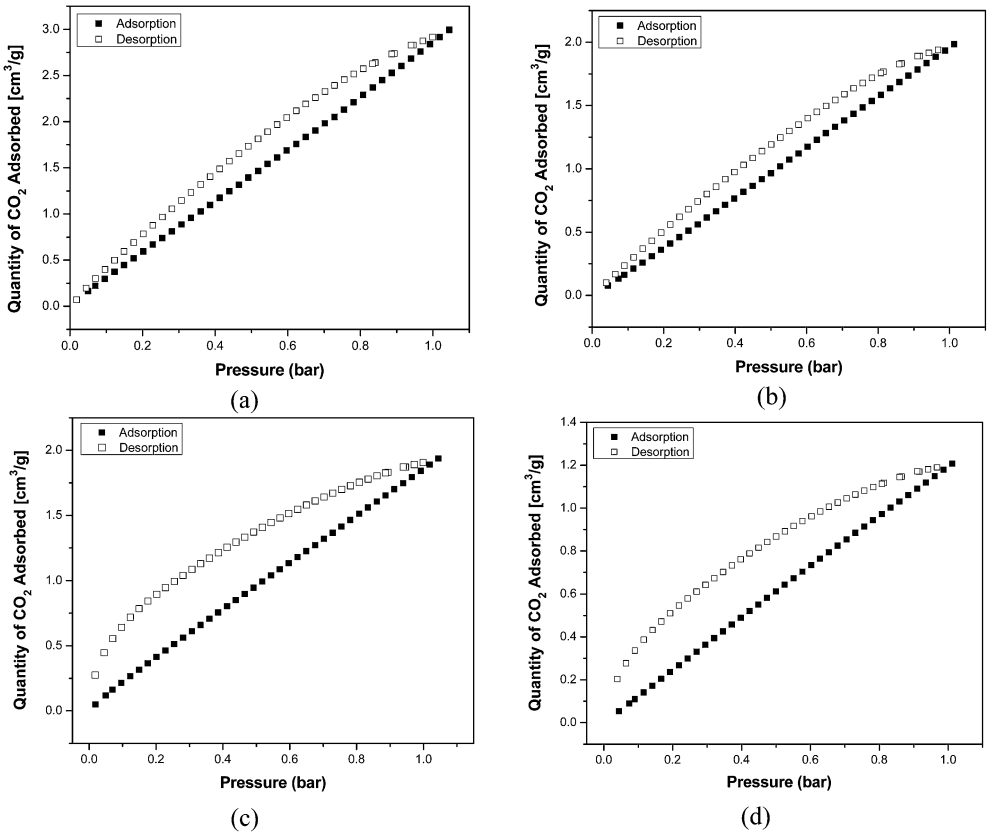

Fig. 5 CO_2 gas sorption isotherms of polyamides at pressure of 1 bar (a) DMAc–NMP at 273 K (b) DMAc–NMP at 298 K and (c) 1,4-dioxane at 273 K (d) 1,4-dioxane at 298 K.

Table 2 CO_2 adsorption capacity of polyamides at 1 bar

	CO_2 adsorbed ($cm^3\ g^{-1}$)		CO_2 adsorbed (mmol g^{-1})	
Polyamide	$T = 273$ K	$T = 298$ K	$T = 273$ K	$T = 298$ K
DMAc–NMP	2.99	1.98	0.134	0.09
1,4-Dioxane	1.94	1.21	0.086	0.054

polyamides probably increases the interaction between basic amide groups and CO_2 molecules. There also exists a strong Lewis acid–base interaction between CO_2 and oxygen of the amide carbonyl as well as π–π interactions with the aromatic phenyl group along with the development of weak H-bonding with phenyl C–H.

The adsorption isotherms of polyamides exhibited "Type-I" behavior at 273 K and 298 K, rendering monolayer adsorption. The adsorption–desorption hysteresis for both the polyamides were observed (Fig. 5). Desorption isotherms remained above the sorption isotherms in both the cases illustrating a significant hysteresis effect associated with the sorption–desorption process. This can either be explained as trapping effect due to interactions of CO_2 with the polymer or due to structural rearrangements. This hysteresis effect revealed that the sorbent/sorbate system is in a metastable state and with the decrease in pressure; the gas is not readily released to the extent corresponding to the thermodynamic equilibrium value. Both polyamides showed significant hysteresis and thus gave large deviations between adsorption and desorption curves. IUPAC gave the empirical classification of hysteresis loop, in which shape of loop is correlated with texture of adsorbent.[43] Polyamides gave H_4 type of hysteresis loops. H_4 loop is usually associated with narrow slit-like pores. The hysteretic adsorption is not reversible because of different adsorption and subsequent desorption isotherms. So, the increased surface area and porosity also led to the superior CO_2 uptake performance of PA-1 compared to PA-2 which clearly rendered DMAc–NMP mixture as better reaction medium relative to 1,4-dioxane.

4. Conclusions

Aromatic polyamides were successfully synthesized from triamine and triacid chloride monomers by solution polymerization in two different solvent systems. The objective of this study was to monitor the effect of solvent used for polymerization on the CO_2 uptake of the polyamides. Polyamides as CO_2 adsorbent demonstrated that they could potentially be exploited for CO_2 capture. The CO_2 adsorption up to 2.99 $cm^3\ g^{-1}$ (0.134 mmol g^{-1}) at 273 K and 1 bar was achieved with polyamide PA-1 which was considerable more relative to the CO_2 adsorption capacity of polyamide PA-2. The higher adsorption by PA-1 ascribed to its

more porous nature and better surface area compared to PA-2. The present study indicated that selection of polymerization solvent was of particular interest and played a very critical role in determining the CO_2 adsorption capacities of the polymers.

Acknowledgements

We are highly thankful for the financial support provided by Korea CCS R&D Centre, Basic Science Research Program through the National Research Foundation of Korea (NRF), ICT & Future Planning (2013R1A1A1012998), and IWT (NRF-2012-C1AAA001-M1A2A2026588).

References

1 S. Choi, J. H. Drese and C. W. Jones, *ChemSusChem*, 2009, **2**, 796–854.
2 Z. J. Liang, M. Marshall and A. L. Chaffee, *Energy Fuels*, 2009, **23**, 2785–2789.
3 E. Dıaz, E. Munoz, A. Vega and S. Ordonez, *Chemosphere*, 2008, **70**, 1375–1382.
4 D. M. D'Alessandro, B. Smit and J. R. Long, *Angew. Chem., Int. Ed.*, 2010, **49**, 6058–6082.
5 R. Baker, *Ind. Eng. Chem. Res.*, 2002, **41**, 1393–1411.
6 M. Gupta, I. Coyle and K. Thambimuthu, Strawman document for CO2 capture and storage (CC&S) technology roadmap, *Proceedings of the 1st CC&S Technology Roadmap Workshop*, Calgary, Alberta, Canada, Sept 18 and 19, 2003.
7 J. D. Figueroa, T. Fout, S. Plasynski, H. McIlvried and R. D. Srivastava, *Int. J. Greenhouse Gas Control*, 2008, **2**, 9–20.
8 M. T. Ho, G. W. Allinson and D. E. Wiley, *Ind. Eng. Chem. Res.*, 2008, **47**, 4883–4890.
9 R. V. Siriwardane, M. S. Shen, E. P. Fisher and J. A. Poston, *Energy Fuels*, 2005, **19**, 1153–1159.
10 F. S. Su, C. S. Lu, S. C. Kuo and W. T. Zeng, *Energy Fuels*, 2010, **24**, 1441–1448.
11 R. V. Siriwardane, M. S. Shen and E. P. Fisher, *Energy Fuels*, 2003, **17**, 571–576.
12 P. D. Jadhav, R. V. Chatti, R. B. Biniwale, N. K. Labhsetwar, S. Devotta and S. S. Rayalu, *Energy Fuels*, 2007, **21**, 3555–3559.
13 R. V. Siriwardane, M. S. Shen, E. P. Fisher and J. Losch, *Energy Fuels*, 2001, **15**, 279–284.
14 J. Prezepiorski, M. Skrodzewicz and A. W. Morawski, *Appl. Surf. Sci.*, 2004, **225**, 235–242.
15 C. Lu, H. Bai, B. Wu, F. Su and J. F. Hwang, *Energy Fuels*, 2008, **22**, 3050–3056.
16 J. S. Baen and S. K. Bhatia, *Energy Fuels*, 2006, **20**, 2599–2607.
17 N. B. McKeown and P. M. Budd, *Chem. Soc. Rev.*, 2006, **35**, 675–683.
18 R. E. Morris and P. S. Wheatley, *Angew. Chem., Int. Ed.*, 2008, **47**, 4966–4981.
19 H. J. Mackintosh, P. M. Budd and N. B. McKeown, *J. Mater. Chem.*, 2008, **18**, 573–578.
20 J. Schmidt, J. Weber, J. D. Epping, M. Antonietti and A. Thomas, *Adv. Mater.*, 2009, **21**, 702–705.
21 A. P. Cote, A. I. Benin, N. W. Ockwig, M. O'Keeffe, A. J. Matzger and O. M. Yaghi, *Science*, 2005, **310**, 1166–1170.
22 H. M. El-Kaderi, J. R. Hunt, J. L. Mendoza-Cortes, A. P. Cote, R. E. Taylor, M. O'Keeffe and O. M. Yaghi, *Science*, 2007, **316**, 268–272.
23 F. J. Uribe-Romo, J. R. Hunt, H. Furukawa, C. Kloeck, M. O'Keeffe and O. M. Yaghi, *J. Am. Chem. Soc.*, 2009, **131**, 4570–4571.
24 P. Kuhn, M. Antonietti and A. Thomas, *Angew. Chem., Int. Ed.*, 2008, **47**, 3450–3453.
25 P. Kuhn, A. Forget, D. Su, A. Thomas and M. Antonietti, *J. Am. Chem. Soc.*, 2008, **130**, 13333–13337.
26 R. Chinchilla and C. Najera, *Chem. Rev.*, 2007, **107**, 874–922.
27 J.-X. Jiang, F. Su, C. D. Wood, N. L. Campbell, H. Niu, C. Dickinson, A. Y. Ganin, M. J. Rosseinsky, Y. Z. Khimyak, A. I. Cooper and A. Trewin, *Angew. Chem., Int. Ed.*, 2007, **46**, 8574–8578.
28 J.-X. Jiang, F. Su, A. Trewin, C. D. Wood, H. Niu, J. T. A. Jones, Y. Z. Khimyak and A. I. Cooper, *J. Am. Chem. Soc.*, 2008, **130**, 7710–7720.
29 J.-X. Jiang, A. Trewin, F. Su, C. D. Wood, H. Niu, Y. Z. Khimyak and A. I. Cooper, *Macromolecules*, 2009, **42**, 2658–2666.
30 T. Ben, H. Ren, S. Ma, D. Cao, J. Lan, X. Jing, W. Wang, J. Xu, F. Deng, J. M. Simmons, S. Qiu and G. Zhu, *Angew. Chem., Int. Ed.*, 2009, **48**, 9457–9460.
31 N. B. McKeown and P. M. Budd, *Macromolecules*, 2010, **43**, 5163–5176.
32 M. P. Tsyurupa and V. A. Davankov, *React. Funct. Polym.*, 2002, **53**, 193–203.
33 J.-H. Ahn, J.-E. Jang, C.-G. Oh, S.-K. Ihm, J. Cortez and D. C. Sherrington, *Macromolecules*, 2006, **39**, 627–632.
34 J. K. Lee, C. D. Wood, D. Bradshaw, M. J. Rosseinsky and A. I. Cooper, *Chem. Commun.*, 2006, 2670–2672.
35 C. D. Wood, B. Tan, A. Trewin, H. Niu, D. Bradshaw, M. J. Rosseinsky, Y. Z. Khimyak, N. L. Campbell, R. Kirk, E. Stoeckel and A. I. Cooper, *Chem. Mater.*, 2007, **19**, 2034–2048.
36 S. Zulfiqar, Z. Ahmad and M. I. Sarwar, *Colloid Polym. Sci.*, 2007, **285**, 1749–1754.
37 S. Zulfiqar, I. Lieberwirth and M. I. Sarwar, *Chem. Phys.*, 2008, **344**, 202–208.
38 S. Zulfiqar and M. I. Sarwar, *High Perform. Polym.*, 2009, **21**, 3–15.
39 S. Zulfiqar, M. Ishaq and M. I. Sarwar, *Adv. Polym. Technol.*, 2010, **29**, 300–308.
40 S. Wan, J. Guo, J. Kim, H. Ihee and D. Jiang, *Angew. Chem., Int. Ed.*, 2008, **47**, 8826–8830.
41 D. M. Ruthven, *Principles of Adsorption and Adsorption Processes*, Wiley, NY, 1984.
42 R. Dawson, D. J. Adams and A. I. Cooper, *Chem. Sci.*, 2011, **2**, 1173–1177.
43 K. S. W. Singh, D. H. Everett, R. A. W. Haul, L. Moscou, R. A. Pierotti and J. Rouquerol, *Pure Appl. Chem.*, 1985, **57**, 603–619.